INTERNATIONAL JOURNAL OF TECHNOLOGY AND ACADEMIC RESEARCH

ISSN: 2224-6878 | Pakistan Volume 6, No. 10.

IF: 14.91 | 2026 http://waerasia.org/index.php/ijtar

# CHANGES IN THE OPTICAL AND MAGNETIC PROPERTIES OF THE $Dy^{3+}$ ION IN $DyAlO_3$ UNDER EXTERNAL INFLUENCES: TEMPERATURE AND MAGNETIC FIELD

**Usmonova Bakhtiniso Sharif qizi**

Lecturer, Department of Exact Sciences,

Bukhara State Technical University, Bukhara, Uzbekistan

usmonova.baxtinis93@gmail.com

**Abstract.** Previous studies of $DyAlO_3$ established the Stark structure of the $Dy^{3+}$ ground multiplet and the Ising character of its ground Kramers doublet, but they did not describe how the optical and magnetic response of the crystal changes when temperature and magnetic field are varied. This work addresses that question. The measured doublet energies (53.7, 125.7 and 205.5 $cm^{-1}$) were combined with the experimentally determined ground-state moment (9.2 ± 0.9 $\mu_B$), the orientation of the moments in the *ab* plane (±33.5° from *b*) and the Néel temperature (3.4 K), and the response to each external influence was calculated with explicit error propagation. The characteristic energies of temperature, field, exchange and crystal field were first placed on one scale, which shows that each influence acts in its own energy window. Temperature changes the ratio of hot to cold absorption lines; choosing the line pair according to the temperature range gives a temperature resolution of 0.05 K at 20 K, 0.2 K at 77 K and 3 K at 300 K for a 1% precision of the measured ratio. The magnetic field splits the ground doublet by 8.6 ± 0.8 $cm^{-1}\cdot T^{-1}$ along the Ising axis. Because the two inequivalent $Dy^{3+}$ sites have different axes, a field in the *ab* plane away from *a* and *b* splits each absorption line into two site components that differ by up to 7.2 $cm^{-1}\cdot T^{-1}$, while the Zeeman components of the Ia and Ib lines cross at 1.27 ± 0.12 T. The effective Verdet constant along *b* deviates by 10% from its weak-field value already at 0.48 T at 4.2 K, but only at about 9 T at 78 K and 34 T at 300 K. A field change of 0–2 T along *b* removes 22.8 (22.0–23.3) $J\cdot kg^{-1}\cdot K^{-1}$ of magnetic entropy at 4.2 K. The Zeeman energy of the moment at the metamagnetic field (3.0 $cm^{-1}$) matches the exchange energy (2.9 $cm^{-1}$). The results give quantitative operating windows for $DyAlO_3$ as a magneto-optical element, a self-referenced optical thermometer and a low-temperature magnetic refrigerant.

**Keywords:** $DyAlO_3$, $Dy^{3+}$, Kramers doublet, Ising anisotropy, Zeeman effect, inequivalent sites, optical thermometry, Faraday effect, metamagnetism, magnetocaloric effect.

**Introduction.** The 4f electrons of a rare-earth ion are shielded by the filled 5s and 5p shells, so the crystal field splits each free-ion multiplet only by a few hundred wavenumbers. These small splittings are comparable with the thermal energy and with the Zeeman energy in laboratory fields. External influences therefore change the optical and magnetic properties of rare-earth crystals strongly: temperature changes which crystal-field states are occupied, and a magnetic field splits these states and polarizes the moments [1]. For a Kramers ion such as $Dy^{3+}$ ($4f^9$), each crystal-field level remains doubly degenerate in any electrostatic field [2], so only the magnetic field can split it. How a level responds to the field is described by its *g*-tensor, which can be extremely anisotropic in a low-symmetry crystal [1].

Dysprosium orthoaluminate $DyAlO_3$ is a model case. Optical studies of the absorption spectrum in magnetic fields showed that the ground doublet of $Dy^{3+}$ carries a moment of 9.2 $\mu_B$

ISSN: 2224-6878 | Pakistan Volume 6, No. 10.

IF: 14.91 | 2026 http://waerasia.org/index.php/ijtar

directed in the *ab* plane at ±33.5° to the *b* axis, that the crystal orders antiferromagnetically at $T_N$ = 3.4 K, and that metamagnetic transitions occur in fields of 7.0 and 7.3 kOe [3]. Magnetic and magnetoelectric measurements confirmed this behaviour [4, 5], and crystal-field analysis linked it to the low ($C_s$) symmetry of the $Dy^{3+}$ site [6]. The Faraday effect was measured between 78 and 300 K along the easy *b* axis, and the Verdet constant was found to follow the magnetic susceptibility [7]. Perovskite $DyAlO_3$ has also been proposed as a magnetic refrigerant for the 4.2–20 K range [8].

Our earlier work on this crystal concentrated on its energy spectrum at zero field. The polarized absorption spectra of the $^6H_{15/2} \rightarrow {}^6F_{3/2}$ band gave the energies of the four lowest Kramers doublets and the $^6F_{3/2}$ splitting [9, 10]. This analysis was used to discuss J-mixing and the polarization selection rules [10], and a separate study built an axial crystal-field model and calculated the zero-field heat capacity and entropy [11]. What these studies did not provide is a quantitative description of how the spectrum and the magnetic response change under external influences, especially for fields of different directions and for the two magnetically inequivalent $Dy^{3+}$ sites. Such a description is needed to choose operating conditions for the applications listed above.

The aim of this work is to determine quantitatively how temperature and magnetic field change the optical and magnetic properties of the $Dy^{3+}$ ion in $DyAlO_3$, using experimentally determined parameters rather than idealized pure-state values. The objectives are:

- to compare the energy scales of the thermal, magnetic, exchange and crystal-field interactions;
- to evaluate the temperature dependence of the hot-to-cold absorption line ratios and the temperature resolution they can provide;
- to calculate the anisotropic and site-resolved Zeeman splitting of the ground doublet and of the absorption lines;
- to determine the field and temperature limits of the linear Faraday response;
- to estimate the field-induced magnetic entropy change and check the consistency of the optical, magnetic and exchange parameters.

**Materials and methods.** *Input data.* $DyAlO_3$ has an orthorhombic distorted-perovskite structure (space group *Pbnm*) with two magnetically inequivalent $Dy^{3+}$ sites whose Ising axes lie in the *ab* plane, symmetric about the *b* axis [3, 6]. Table 1 lists the parameters used. The doublet energies were obtained from the eight Stark components of the $^6H_{15/2} \rightarrow {}^6F_{3/2}$ band recorded in polarized light [9, 10]. The moment, its orientation, the Néel temperature, the exchange energy and the metamagnetic fields come from optical and Zeeman measurements [3]. The Landé factor of the $^6F_{3/2}$ multiplet was calculated in the LS-coupling approximation ($S$ = 5/2, $L$ = 3, $J$ = 3/2), which gives $g_J$ = 16/15.

**Table 1.** Experimental parameters of the $Dy^{3+}$ ion in $DyAlO_3$ used in the analysis

| Parameter | Value | Source |
|---|---|---|
| Energies of Kramers doublets II, III, IV of $^6H_{15/2}$ | 53.7 ± 0.9; 125.7 ± 0.9; 205.5 ± 0.3 $cm^{-1}$ | [9, 10] |

ISSN: 2224-6878 | Pakistan Volume 6, No. 10.

IF: 14.91 | 2026 http://waerasia.org/index.php/ijtar

| Parameter | Value | Source |
|---|---|---|
| Energies of the Ia and Ib lines | 13 293.7 and 13 304.6 $cm^{-1}$ | [9] |
| Ground-state moment μ | (9.2 ± 0.9) $\mu_B$; $g_{\parallel} = 2\mu/\mu_B = 18.4 \pm 1.8$ | [3] |
| Orientation of the Ising axes | *ab* plane, ±33.5° from the *b* axis | [3] |
| Néel temperature $T_N$ | 3.4 K | [3] |
| Exchange energy along *c*, $W_C$ | −(2.9 ± 0.6) $cm^{-1}$ | [3] |
| Metamagnetic fields (*H* parallel to the moments) | 7.0 and 7.3 kOe | [3] |
| Landé factor of $^6F_{3/2}$ | 16/15 ≈ 1.067 | calculated |
| Molar mass of $DyAlO_3$ | 237.48 $g \cdot mol^{-1}$ | calculated |

*Source: compiled by the author.*

*Temperature response.* The ratio of the intensity of a hot line starting from doublet *K* to that of the corresponding cold line starting from doublet I was described by the Boltzmann factor, assuming equal oscillator strengths. Its relative thermal sensitivity $S_r$, the standard figure of merit of lanthanide thermometers [12], is

$$R_K(T)=exp(-\frac{\Delta_K}{k_BT}), \qquad S_r=\frac{1}{R_K}|\frac{dR_K}{dT}|=\frac{\Delta_K}{k_BT^2}, \qquad \delta T=\frac{\delta R/R}{S_r}, \tag{1}$$

where $k_B$ = 0.6950 $cm^{-1} \cdot K^{-1}$ and $\delta T$ is the temperature resolution for a relative precision $\delta R/R$ of the measured ratio. A ratio was considered measurable if $R_K \geq 0.01$, and for each temperature the line pair with the highest $S_r$ that meets this condition was selected.

*Field response.* For an Ising doublet ($g_{\perp} \approx 0$) [1], a field *B* in the *ab* plane at angle ψ to the *b* axis splits the ground doublets of the two sites by

$$\Delta E_{1,2}=g_{\parallel}\mu_B B|cos(\psi \mp \theta)|, \qquad \theta=33.5°, \tag{2}$$

with $\mu_B$ = 0.4669 $cm^{-1} \cdot T^{-1}$. For a field along *b* (ψ = 0°) or *a* (ψ = 90°), both sites have the same splitting; for any other direction in the *ab* plane, they differ. An absorption line between a ground doublet with $g_g$ and an excited doublet with $g_e$ splits into components at

$$E=E_0 \pm \frac{1}{2}(g_g \pm g_e)\mu_B B. \tag{3}$$

*Faraday response and magnetic entropy.* Above $T_N$, with only the ground doublet populated, the moment along the field is $M = ½g_{eff}\mu_B \tanh x$, where $x = g_{eff}\mu_B B/(2k_B T)$. Since the paramagnetic Faraday rotation is proportional to the magnetization [7], the effective Verdet constant $\theta_F/(BL)$ changes with the field as

ISSN: 2224-6878 | Pakistan Volume 6, No. 10.

IF: 14.91 | 2026 http://waerasia.org/index.php/ijtar

$$\frac{V_{eff}(B)}{V_0}=\frac{\tanh x}{x}, \qquad -\Delta S_M=R\ ln\ 2-R[ln(2cosh\ x)-x\ tanh\ x]. \tag{4}$$

The second expression gives the isothermal magnetic entropy change for a field change from 0 to $B$ [13, 14]. The field $B_{10\%}$ at which $V_{\text{eff}}$ deviates by 10% from $V_0$ ($x$ = 0.584) was taken as the upper limit of the linear Faraday regime. Uncertainties were propagated from the error of $g_{//}$ (±10%), which dominates over the errors of the doublet energies. The model neglects exchange above $T_N$, the van Vleck contribution and the excited doublets, so the field-response results are quantitative between $T_N$ and about 30 K, where more than 92% of the ions are in the ground doublet, and indicative at higher temperatures.

**Results.** *Hierarchy of energy scales.* Table 2 and Figure 1 place all interactions of $Dy^{3+}$ in $DyAlO_3$ on one energy scale. The exchange energy and the thermal energy at $T_N$ are the smallest, 2–3 $cm^{-1}$. The Zeeman splitting at 1 T along the Ising axis (8.6 $cm^{-1}$) is close to the $^6F_{3/2}$ splitting (10.1–10.9 $cm^{-1}$), and at 5 T (43 $cm^{-1}$) it approaches the energy of doublet II. The thermal energy at 77 K almost equals the energy of doublet II, and at 300 K that of doublet IV. The field therefore acts mainly within a doublet, while temperature acts between doublets, and the two influences can be analysed separately.

**Table 2.** Energy scales of the interactions of the $Dy^{3+}$ ion in $DyAlO_3$

| Interaction | Energy, $cm^{-1}$ | Equivalent temperature, K | What it changes |
|---|---|---|---|
| Thermal energy at $T_N$ = 3.4 K | 2.36 | 3.4 | onset of antiferromagnetic order |
| Exchange along $c$, $\|W_C\|$ | 2.9 | 4.2 | magnetic order, metamagnetism |
| Zeeman splitting, 1 T along the Ising axis | 8.6 ± 0.8 | 12.4 | splitting of the ground doublet |
| $^6F_{3/2}$ splitting δ | 10.1–10.9 | 14.5–15.7 | spacing of lines a and b |
| Thermal energy at 20 K | 13.9 | 20 | first hot lines appear |
| Zeeman splitting, 5 T along the Ising axis | 43 ± 4 | 62 | field-induced line crossings |
| Thermal energy at 77 K | 53.5 | 77 | hot lines comparable with cold ones |
| Doublet II | 53.7 | 77.3 | first hot band |
| Doublet IV | 205.5 | 295.7 | hot bands at room temperature |

ISSN: 2224-6878 | Pakistan Volume 6, No. 10.

IF: 14.91 | 2026 http://waerasia.org/index.php/ijtar

| Interaction | Energy, $cm^{-1}$ | Equivalent temperature, K | What it changes |
|---|---|---|---|
| Thermal energy at 300 K | 208.5 | 300 | all four doublets populated |

*Source: calculated by the author from the data of Table 1.*

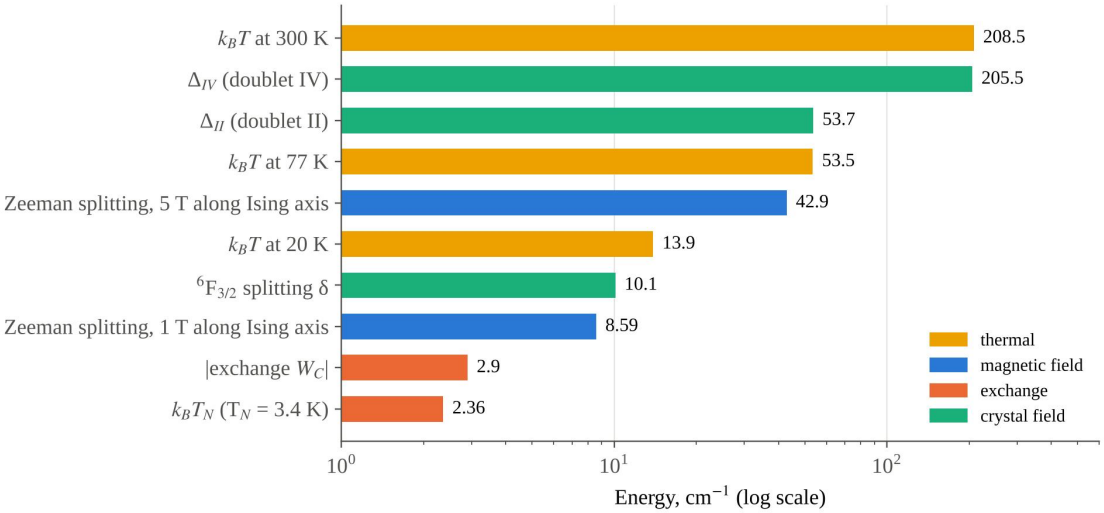



***Figure 1.*** *Energy scales of thermal, magnetic, exchange and crystal-field interactions of $Dy^{3+}$ in $DyAlO_3$ (logarithmic axis). Calculated by the author.*

*Temperature response of the absorption spectrum.* Figure 2a shows how the hot-to-cold line ratios grow with temperature. The II/I ratio reaches 0.01 at about 17 K, the III/I ratio at about 40 K and the IV/I ratio at about 64 K, so the hot lines become measurable one after another as the temperature rises. The relative sensitivity (Figure 2b, Table 3) falls as $1/T^2$ and is larger for higher-lying doublets. The two trends work against each other: a high-lying doublet gives a more sensitive ratio but a weaker hot line. Selecting the pair with the highest sensitivity among the measurable ones gives the temperature resolution shown in the last column of Table 3. For a ratio measured with 1% precision, the resolution is 0.05 K at 20 K, 0.2 K at 77 K and 3 K at 300 K.

**Table 3.** Hot-to-cold line ratios, their thermal sensitivity and the attainable temperature resolution

| $T$, K | $R_{II}$ | $R_{III}$ | $R_{IV}$ | $S_r$: II/I; III/I; IV/I, %·$K^{-1}$ | Best pair ($R$ ≥ 0.01) | δ$T$ at δ$R/R$ = 1%, K |
|---|---|---|---|---|---|---|
| 20 | 0.021 | $1.2\times10^{-4}$ | $3.8\times10^{-7}$ | 19.3; 45.2; 73.9 | II/I | 0.05 |
| 50 | 0.213 | 0.027 | 0.0027 | 3.09; 7.23; 11.8 | III/I | 0.14 |
| 77 | 0.367 | 0.095 | 0.022 | 1.30; 3.05; 4.99 | IV/I | 0.20 |
| 150 | 0.597 | 0.299 | 0.139 | 0.34; 0.80; 1.31 | IV/I | 0.76 |

ISSN: 2224-6878 | Pakistan Volume 6, No. 10.

IF: 14.91 | 2026 http://waerasia.org/index.php/ijtar

| $T$, K | $R_{II}$ | $R_{III}$ | $R_{IV}$ | $S_r$: II/I; III/I; IV/I, %·K$^{-1}$ | Best pair ($R \geq 0.01$) | $\delta T$ at $\delta R/R$ = 1%, K |
|---|---|---|---|---|---|---|
| 300 | 0.773 | 0.547 | 0.373 | 0.09; 0.20; 0.33 | IV/I | 3.0 |

*Source: calculated by the author with Eq. (1), assuming equal oscillator strengths of hot and cold lines.*

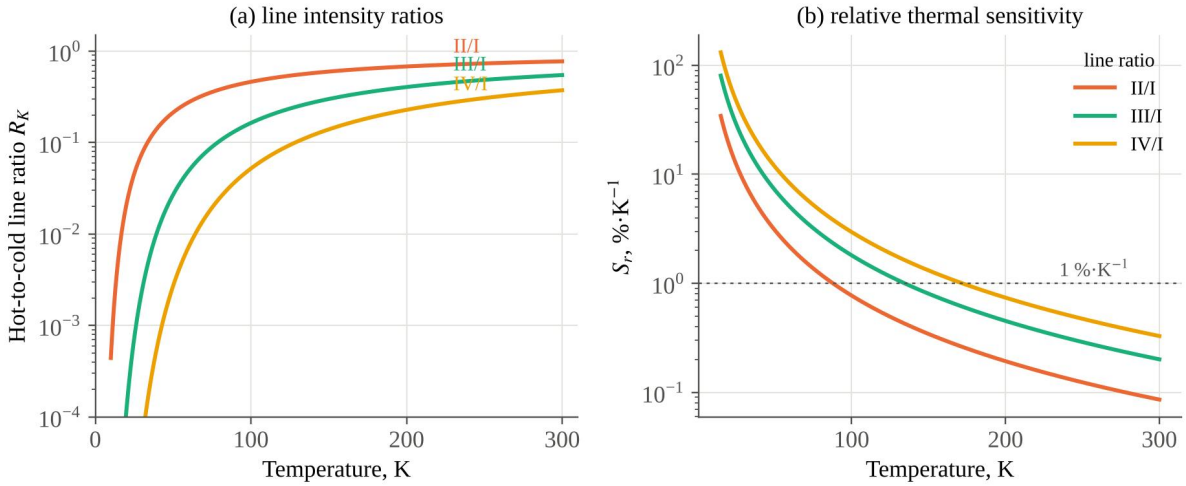



***Figure 2.*** *Temperature response of the $^6H_{15/2} \rightarrow {}^6F_{3/2}$ band: (a) hot-to-cold line intensity ratios; (b) relative thermal sensitivity. Calculated by the author.*

*Anisotropic and site-resolved Zeeman splitting.* Table 4 gives the Zeeman parameters of the ground doublet for the principal field directions. The splitting is 8.6 ± 0.8 cm$^{-1}$·T$^{-1}$ along the Ising axis, 7.2 ± 0.7 along *b*, 4.7 ± 0.5 along *a* and practically zero along *c*. The ratio of the Curie susceptibilities along *b* and *a* is therefore $\cot^2 33.5° = 2.28$, which explains why *b* is the easy-magnetization axis [7].

**Table 4.** Zeeman parameters of the ground Kramers doublet of $Dy^{3+}$ for the principal field directions

| Field direction | $g_{eff}$ | Splitting, cm$^{-1}$·T$^{-1}$ | $M_{sat}$, $\mu_B$ | Relative $\chi$ (Curie term) | Ia/Ib crossing field, T | $B_{10\%}$ at 4.2 K, T | $B_{10\%}$ at 300 K, T |
|---|---|---|---|---|---|---|---|
| Ising axis | 18.4 | 8.59 ± 0.84 | 9.20 | 1.00 | 1.27 ± 0.12 | 0.40 | 28 |
| *b* axis | 15.3 | 7.16 ± 0.70 | 7.67 | 0.70 | 1.52 ± 0.15 | 0.48 | 34 |
| *a* axis | 10.2 | 4.74 ± 0.46 | 5.08 | 0.30 | 2.30 ± 0.22 | 0.72 | 51 |
| *c* axis | ≈ 0 | ≈ 0 | ≈ 0 | ≈ 0 | — | — | — |

ISSN: 2224-6878 | Pakistan Volume 6, No. 10.

IF: 14.91 | 2026 http://waerasia.org/index.php/ijtar

*Source: calculated by the author with Eqs. (2)–(4); $B_{10\%}$ is the field at which the effective Verdet constant deviates by 10% from its weak-field value; the 300 K values neglect excited doublets and are indicative.*

The two inequivalent sites add a feature that does not appear for fields along the crystal axes. When the field is turned in the *ab* plane away from *a* and *b*, the two sites have different projections of their Ising axes on the field, Eq. (2). Figure 3 and Table 5 show the result. At ψ = 0° and 90° both sites split equally. In between, the splittings differ, and the difference reaches 7.2 $cm^{-1}·T^{-1}$ near ψ = 60°, where the field is almost perpendicular to the axis of site 2 (at ψ = 56.5° the site-2 doublet does not split at all). In this geometry each Zeeman component of the absorption lines appears twice, once for each site. The site doubling offers a direct optical way to measure the angle θ: the field direction at which the splitting of one site vanishes equals 90° − θ.

**Table 5.** Splitting of the ground doublets of the two inequivalent sites for a field in the *ab* plane ($cm^{-1}·T^{-1}$)

| ψ, deg | 0 (*b*) | 15 | 30 | 45 | 60 | 75 | 90 (*a*) |
|---|---|---|---|---|---|---|---|
| Site 1 (axis at +33.5°) | 7.16 | 8.15 | 8.57 | 8.42 | 7.69 | 6.43 | 4.74 |
| Site 2 (axis at −33.5°) | 7.16 | 5.69 | 3.83 | 1.71 | 0.52 | 2.73 | 4.74 |
| **Difference** | **0** | **2.45** | **4.74** | **6.71** | **7.16** | **3.71** | **0** |

*Source: calculated by the author with Eq. (2), $g_{/\!/} = 18.4$.*

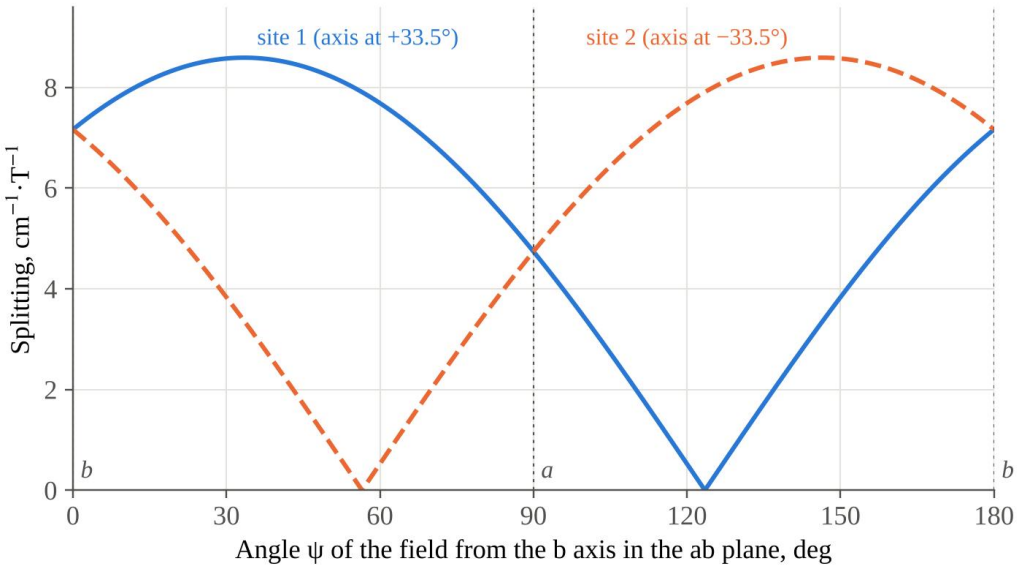



***Figure 3.*** *Zeeman splitting of the ground doublets of the two inequivalent $Dy^{3+}$ sites as a function of the field direction in the ab plane. Calculated by the author.*

*Field response of the absorption lines.* The $^6F_{3/2}$ sublevels have much smaller *g*-values than the ground doublet: in the pure-state approximation 3.2 for $|\pm 3/2\rangle$ and 1.07 for $|\pm 1/2\rangle$, so their splitting does not exceed 1.5 $cm^{-1}·T^{-1}$, about one sixth of that of the ground doublet.

ISSN: 2224-6878 | Pakistan Volume 6, No. 10.

IF: 14.91 | 2026 http://waerasia.org/index.php/ijtar

According to Eq. (3), the Zeeman pattern of the absorption lines is therefore controlled by the ground doublet, and magneto-absorption measures the ground-state moment directly [3]. Figure 4 shows the pattern of the Ia and Ib lines for a field along the Ising axis. The upper component of Ia and the lower component of Ib approach each other at 8.6 $cm^{-1} \cdot T^{-1}$ and cross at 1.27 ± 0.12 T. For fields along *b* and *a* the crossing moves to 1.52 and 2.30 T (Table 4). Above these fields the order of the components no longer follows the order of the $^6F_{3/2}$ sublevels, which must be taken into account when lines are assigned in Zeeman spectra.

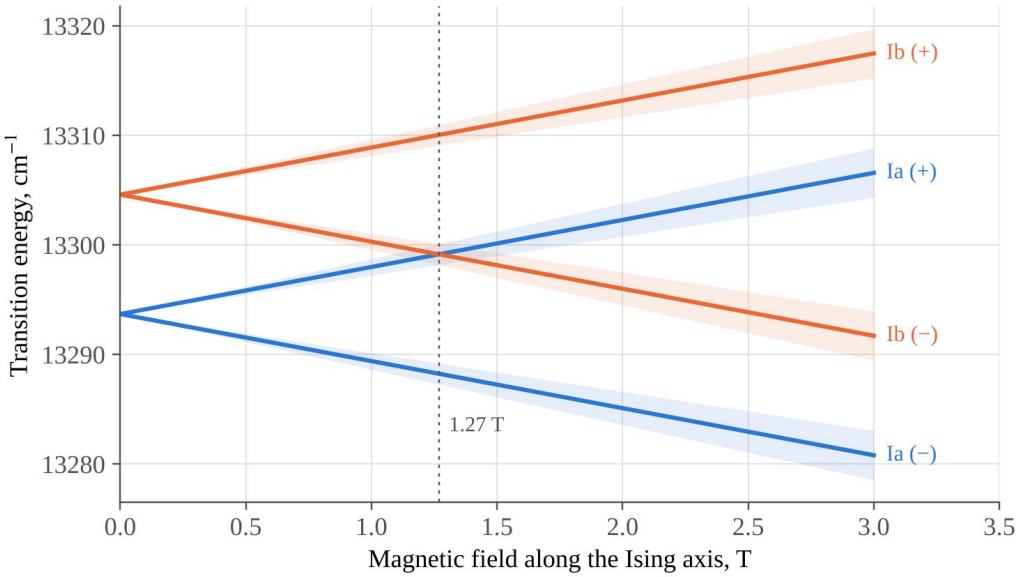



***Figure 4.*** *Zeeman pattern of the Ia and Ib absorption lines for a field along the Ising axis. Lines show the contribution of the ground doublet; shaded bands show the maximum additional splitting of the $^6F_{3/2}$ sublevels. Calculated by the author.*

*Linear and nonlinear Faraday response.* Table 6 and Figure 5 show how the effective Verdet constant along *b* changes with the field, Eq. (4). At 4.2 K it falls to 0.69 of its weak-field value at 1 T and to 0.16 at 5 T, and the 10% deviation is reached already at 0.48 T. The linear range grows in proportion to temperature: $B_{10\%}$ is 1.1 T at 10 K, 2.3 T at 20 K and 3.4 T at 30 K. Extrapolated to higher temperatures, it reaches about 9 T at 78 K and 34 T at 300 K. This explains why the Verdet constant measured between 78 and 300 K in ordinary laboratory fields is field-independent and follows the susceptibility [7]. At helium temperatures, in contrast, the Faraday rotation of $DyAlO_3$ is nonlinear in any useful field, and the measured Verdet constant depends on the field used.

**Table 6.** Effective Verdet constant along the *b* axis relative to its weak-field value, $V_{eff}/V_0$

| ***T*, K** | **0.5 T** | **1 T** | **2 T** | **5 T** | **$B_{10\%}$, T** |
|---|---|---|---|---|---|
| 4.2 | 0.891 | 0.686 | 0.402 | 0.163 | 0.48 |
| 10 | 0.978 | 0.920 | 0.751 | 0.384 | 1.13 |
| 20 | 0.995 | 0.978 | 0.920 | 0.667 | 2.27 |

ISSN: 2224-6878 | Pakistan Volume 6, No. 10.

IF: 14.91 | 2026 http://waerasia.org/index.php/ijtar

| *T*, K | 0.5 T | 1 T | 2 T | 5 T | $B_{10\%}$, T |
|---|---|---|---|---|---|
| 30 | 0.998 | 0.990 | 0.962 | 0.810 | 3.40 |

*Source: calculated by the author with Eq. (4), $g_{eff}$ = 15.3.*

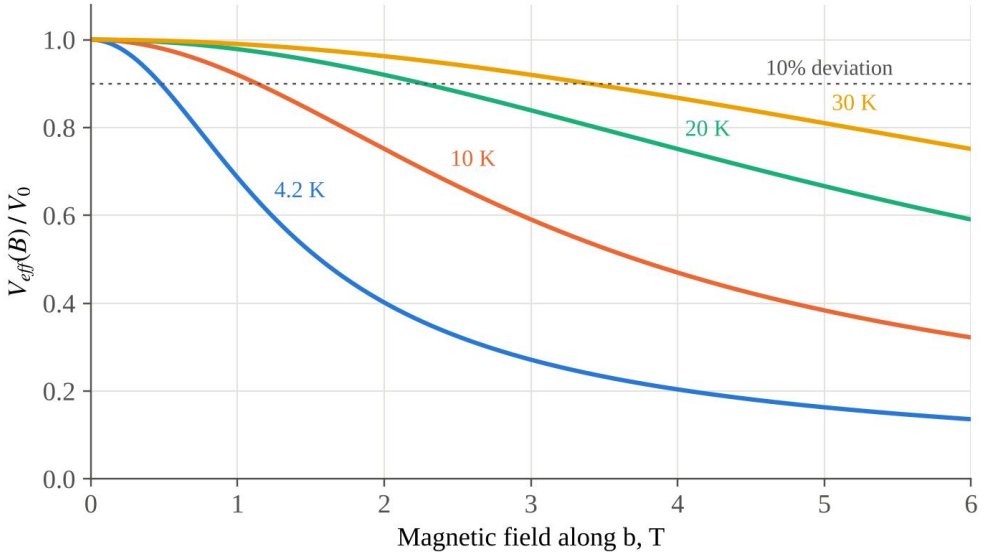



***Figure 5.*** *Field dependence of the effective Verdet constant of $DyAlO_3$ along the b axis at 4.2, 10, 20 and 30 K. Calculated by the author.*

*Field-induced magnetic entropy change.* Table 7 and Figure 6 give the isothermal entropy change for field changes up to 5 T. At 4.2 K a field of 2 T along *b* removes 22.8 $J \cdot kg^{-1} \cdot K^{-1}$, which is 94% of the doublet limit $R \ln 2 = 24.3$ $J \cdot kg^{-1} \cdot K^{-1}$. With the ±10% uncertainty of $g_{//}$, the value lies between 22.0 and 23.3 $J \cdot kg^{-1} \cdot K^{-1}$. The response decreases quickly with temperature: at 20 K a field of 2 T gives 4.1 (3.4–4.8) $J \cdot kg^{-1} \cdot K^{-1}$, and 5 T is needed for 15.3 $J \cdot kg^{-1} \cdot K^{-1}$. The field direction matters: along *a*, the entropy change at 10 K and 2 T is 6.6 $J \cdot kg^{-1} \cdot K^{-1}$, 55% of the value along *b*.

**Table 7.** Magnetic entropy change $-\Delta S_M$ ($J \cdot kg^{-1} \cdot K^{-1}$) of $DyAlO_3$ in the Ising-doublet model

| *T*, K | *b*: 0→1 T | *b*: 0→2 T | *b*: 0→5 T | Ising axis: 0→2 T | *a*: 0→2 T |
|---|---|---|---|---|---|
| 4.2 | 14.6 | 22.8 (22.0–23.3) | 24.3 | 23.6 | 18.7 |
| 10 | 4.1 | 11.9 (10.4–13.3) | 23.0 | 14.7 | 6.6 |
| 20 | 1.1 | 4.1 (3.4–4.8) | 15.3 | 5.6 | 1.9 |
| 30 | 0.5 | 2.0 | 9.3 | 2.7 | 0.9 |

*Source: calculated by the author with Eq. (4); ranges correspond to $g_{//} = 18.4 \pm 1.8$; exchange and lattice contributions are neglected.*

ISSN: 2224-6878 | Pakistan Volume 6, No. 10.

IF: 14.91 | 2026 http://waerasia.org/index.php/ijtar

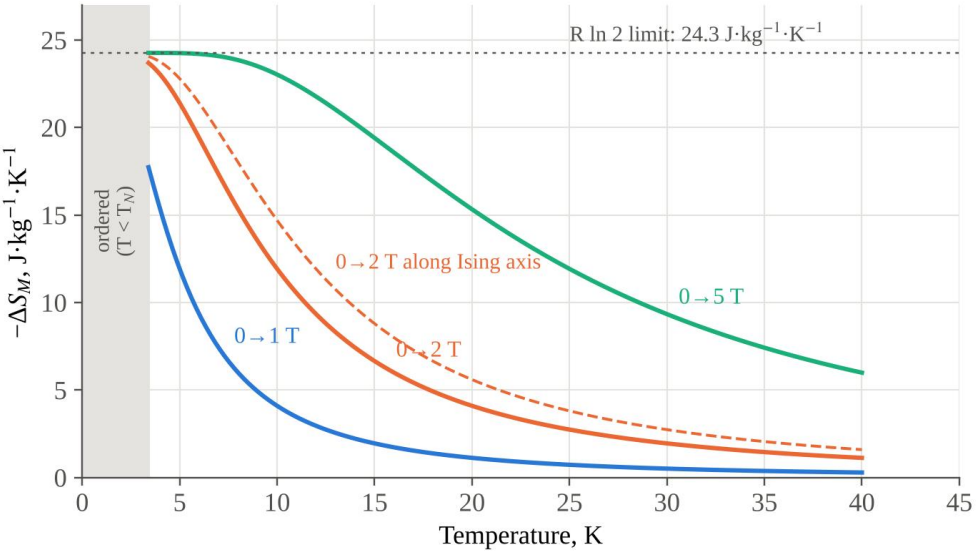



***Figure 6.*** *Field-induced magnetic entropy change of $DyAlO_3$ for field changes along b (solid) and along the Ising axis (dashed) above $T_N$. Calculated by the author.*

*Consistency of the optical, magnetic and exchange parameters.* Table 8 compares quantities obtained in different experiments. The Zeeman energy of a 9.2 $\mu_B$ moment in the metamagnetic field of 0.70 T is 3.0 $cm^{-1}$, which agrees with the exchange energy along *c* found from line shifts, 2.9 ± 0.6 $cm^{-1}$ [3]. The thermal energy at $T_N$ is of the same order (2.4 $cm^{-1}$). The metamagnetic transition thus occurs when the Zeeman energy of a moment becomes equal to its exchange energy, as expected for an Ising antiferromagnet. The measured moment also gives a quantitative measure of the purity of the ground doublet: it corresponds to $\langle J_z \rangle = 6.9$, i.e. 92% of the value for a pure $|\pm 15/2\rangle$ state. The ideal value $g_{\parallel} = 20$ used in zero-field models [10, 11] is thus an upper bound, and the ground doublet contains admixtures of states with smaller $|M_J|$.

**Table 8.** Consistency check of independently determined parameters

| Quantity | Value | Basis |
|---|---|---|
| Zeeman energy $\mu B_c$ at $B_c$ = 0.70 T | 3.0 $cm^{-1}$ | 9.2 $\mu_B$ × 0.70 T [3] |
| Exchange energy along *c*, $\lvert W_C \rvert$ | 2.9 ± 0.6 $cm^{-1}$ | line shifts below $T_N$ [3] |
| Thermal energy $k_B T_N$ | 2.36 $cm^{-1}$ | $T_N$ = 3.4 K [3] |
| Splitting of the ground doublet at $B_c$ | 6.0 $cm^{-1}$ | $g_{\parallel}$ = 18.4, Eq. (2) |
| $\langle J_z \rangle$ of the ground doublet / (15/2) | 0.92 | $g_{\parallel}/(2g_J) = 6.9$ |

*Source: calculated by the author.*

**Discussion.** *What is new compared with zero-field studies.* The previous analyses of $DyAlO_3$ described the energy spectrum, the polarization selection rules and the zero-field thermodynamics of $Dy^{3+}$ [10, 11] and used the idealized $|\pm 15/2\rangle$ ground doublet. The present

ISSN: 2224-6878 | Pakistan Volume 6, No. 10.

IF: 14.91 | 2026 http://waerasia.org/index.php/ijtar

work moves to the response of the crystal to temperature and field and replaces the idealized parameters by measured ones ($g_{//}$ = 18.4 instead of 20, the axis angle 33.5°). Four results follow that the zero-field picture cannot give: the attainable temperature resolution of the line-ratio thermometer, the site-resolved Zeeman pattern for arbitrary field directions in the *ab* plane, the field limits of the linear Faraday response, and the field-induced entropy change with its uncertainty.

*Temperature.* The temperature acts through the occupation of the Kramers doublets, and the hot-to-cold line ratios turn the absorption spectrum into an internal thermometer. Because the higher doublets give more sensitive but weaker lines, the best line pair changes with temperature: II/I below about 40 K, III/I between 40 and 65 K and IV/I above 65 K. With this choice the sensitivity stays above 1%·K$^{-1}$, the usual benchmark for lanthanide thermometers [12], up to about 170 K. Such a thermometer is useful in magneto-optical and magnetocaloric experiments, where the sample temperature can differ from that of the holder because of optical heating or adiabatic demagnetization.

*Magnetic field.* The Ising character of the ground doublet makes the Zeeman effect extremely anisotropic, from 8.6 cm$^{-1}$·T$^{-1}$ along the local axis to practically zero along *c*. The existence of two sites with different axes has a practical consequence for spectroscopy. Fields along *a* or *b* give simple spectra with one set of Zeeman components, whereas fields at intermediate angles double every component. Measuring the angle at which one site stops splitting gives the axis angle θ independently of neutron or Mössbauer data. The same angle sets the polarization ratio of π- and σ-type transitions in the two-site model of the polarized spectra ($\cot^2 \theta = 2.28$) [10], so the optical, magnetic and magneto-optical anisotropies of $DyAlO_3$ are all controlled by one geometric parameter.

*Applications.* For magneto-optics, the main result is the crossover from linear to saturated Faraday response. At 78–300 K, the Verdet constant is field-independent up to several tesla [7], so $DyAlO_3$ can serve as a linear Faraday element. At 4.2 K the rotation saturates above about 0.5 T, and the element works as a saturated rotator whose angle is set by the moment rather than by the field. For magnetic cooling, the results agree with the view that $DyAlO_3$ is a promising refrigerant for 4.2–20 K [8]: almost the whole doublet entropy is removed by 2 T along *b* at 4.2 K, because doublet II lies 77 K above the ground doublet and does not take part. The anisotropy requires oriented crystals with the field along *b*. Close to $T_N$, the paramagnetic model overestimates the effect, because short-range antiferromagnetic correlations already reduce the entropy [13, 14].

*Other external influences.* Hydrostatic pressure or uniaxial stress would change the crystal-field parameters and therefore the doublet energies $\Delta_K$. According to Eq. (1), a shift of only 1 cm$^{-1}$ in $\Delta_{II}$ changes $R_{II}$ by 1.9% at 77 K and by 7% at 20 K, so the line-ratio method could also detect strain-induced changes of the crystal field. These effects were not quantified here because no pressure data for $DyAlO_3$ are available.

*Limitations.* The field-response calculations treat each $Dy^{3+}$ ion as an isolated Ising doublet. They neglect exchange above $T_N$, the van Vleck contribution and the excited doublets, so they are quantitative between about 4 and 30 K and indicative at higher temperatures. The *g*-values of the $^6F_{3/2}$ sublevels were estimated for pure states. The line-ratio analysis assumes equal oscillator strengths of hot and cold lines, which must be checked experimentally. Temperature-

ISSN: 2224-6878 | Pakistan Volume 6, No. 10.

IF: 14.91 | 2026 http://waerasia.org/index.php/ijtar

resolved absorption between 4.2 and 300 K, magneto-absorption in fields up to 5 T with rotation in the *ab* plane, and magnetization or heat-capacity measurements in field are the natural tests of these predictions.

**Conclusion.** The analysis of the response of the $Dy^{3+}$ ion in $DyAlO_3$ to temperature and magnetic field leads to the following conclusions:

1. Temperature and field act in separate energy windows: the field splits Kramers doublets by up to 8.6 ± 0.8 $cm^{-1}\cdot T^{-1}$, temperature redistributes ions between doublets separated by 53.7–205.5 $cm^{-1}$, and exchange (2.9 $cm^{-1}$) matters only near $T_N$ = 3.4 K.
2. The hot-to-cold line ratios of the $^6H_{15/2} \rightarrow {}^6F_{3/2}$ band form an internal thermometer. With the line pair chosen according to the temperature, a 1% ratio precision gives a resolution of 0.05 K at 20 K, 0.2 K at 77 K and 3 K at 300 K.
3. The Zeeman splitting of the ground doublet is 8.6, 7.2 and 4.7 $cm^{-1}\cdot T^{-1}$ along the Ising axis, *b* and *a*, and practically zero along *c*. For fields in the *ab* plane away from *a* and *b*, the two inequivalent sites split differently, by up to 7.2 $cm^{-1}\cdot T^{-1}$, and the components of lines Ia and Ib cross at 1.27–2.30 T depending on the field direction.
4. The Faraday response along *b* is linear within 10% only below 0.48 T at 4.2 K, but up to about 9 T at 78 K and 34 T at 300 K.
5. A field change of 0–2 T along *b* removes 22.8 (22.0–23.3) $J\cdot kg^{-1}\cdot K^{-1}$ of magnetic entropy at 4.2 K and 4.1 (3.4–4.8) $J\cdot kg^{-1}\cdot K^{-1}$ at 20 K. The Zeeman energy at the metamagnetic field (3.0 $cm^{-1}$) agrees with the exchange energy (2.9 $cm^{-1}$), and the measured moment corresponds to a ground doublet that is 92% $|\pm 15/2\rangle$ .

These results define the conditions under which $DyAlO_3$ can serve as a linear or saturated Faraday element, a self-referenced optical thermometer and a magnetic refrigerant for the 4.2–20 K range.

## REFERENCES

1. Abragam A., Bleaney B. Electron Paramagnetic Resonance of Transition Ions. Oxford: Clarendon Press, 1970. 911 p.
2. Kramers H.A. Théorie générale de la rotation paramagnétique dans les cristaux // Proceedings of the Royal Netherlands Academy of Arts and Sciences. 1930. Vol. 33. P. 959–972.
3. Schuchert H., Hüfner S., Faulhaber R. Optical investigation of metamagnetic $DyAlO_3$ // Zeitschrift für Physik. 1969. Vol. 222, No. 2. P. 105–127. DOI: 10.1007/BF01392289.
4. Holmes L.M., Van Uitert L.G., Hecker R.R., Hull G.W. Magnetic behavior of metamagnetic $DyAlO_3$ // Physical Review B. 1972. Vol. 5, No. 1. P. 138–146. DOI: 10.1103/PhysRevB.5.138.
5. Holmes L.M., Van Uitert L.G. Magnetoelectric effect and metamagnetic transitions in $DyAlO_3$ // Physical Review B. 1972. Vol. 5, No. 1. P. 147–153. DOI: 10.1103/PhysRevB.5.147.
6. Kolmakova N.P., Krynetskii I.B., Lukina M.M., et al. Crystal field and metamagnetic behavior of rare-earth orthoaluminates: $DyAlO_3$ // Physica Status Solidi (b). 1990. Vol. 159, No. 2. P. 465–474. DOI: 10.1002/pssb.2221590217.

ISSN: 2224-6878 | Pakistan Volume 6, No. 10.

IF: 14.91 | 2026 http://waerasia.org/index.php/ijtar

7. Valiev U.V., Malysheva M.E., Rakhimov Sh.A., Sultonov O.Z. Features of the Faraday effect in the rare earth orthoaluminate $DyAlO_3$ // Optics and Spectroscopy. 2022. Vol. 130, No. 4. P. 295–301. DOI: 10.1134/S0030400X22040117.
8. Kuz'min M.D., Tishin A.M. Magnetic refrigerants for the 4.2–20 K region: garnets or perovskites? // Journal of Applied Physics. 1993. Vol. 73, No. 9. P. 4083–4086.
9. Valiev U.V., Dzhuraev D.R., Malyshev E.E., Saidov K.S. Electronic structure of the ground multiplet of the $Dy^{3+}$ ion in $DyAlO_3$ orthoaluminate // Optika i Spektroskopiya. 1999. Vol. 86, No. 5. P. 789–793 (in Russian).
10. Brites C.D.S., Balabhadra S., Carlos L.D. Lanthanide-based thermometers: at the cutting-edge of luminescence thermometry // Advanced Optical Materials. 2019. Vol. 7, No. 5. Article 1801239.
11. Tishin A.M., Spichkin Y.I. The Magnetocaloric Effect and its Applications. Bristol: Institute of Physics Publishing, 2003. 476 p.
12. Pecharsky V.K., Gschneidner K.A. Jr. Magnetocaloric effect and magnetic refrigeration // Journal of Magnetism and Magnetic Materials. 1999. Vol. 200, No. 1–3. P. 44–56.